



## Osseointegration of titanium with an antimicrobial nanostructured noble metal coating

Sara Svensson, MSc<sup>a,b,\*</sup>, Felicia Suska, DDS, PhD<sup>a,b</sup>, Lena Emanuelsson, BSc<sup>a,b</sup>, Anders Palmquist, PhD<sup>a,b</sup>, Birgitta Norlindh, BSc<sup>a,b</sup>, Margarita Trobos, PhD<sup>a,b</sup>, Helen Bäckros, MSc<sup>a,c</sup>, Linda Persson, MSc<sup>a,c</sup>, Gunilla Rydja, MSc<sup>a,c</sup>, Mattias Ohrlander, PhD<sup>a,c</sup>, Benny Lyvén, PhD<sup>a,d</sup>, Jukka Lausmaa, PhD<sup>a,d</sup>, Peter Thomsen, MD, PhD<sup>a,b</sup>

<sup>a</sup>BIOMATCELL VINN Excellence Center of Biomaterials and Cell Therapy, Göteborg, Sweden

<sup>b</sup>Department of Biomaterials, Sahlgrenska Academy at University of Gothenburg, Göteborg, Sweden

<sup>c</sup>Bactiguard AB, Stockholm, Sweden

<sup>d</sup>SP Technical Research Institute of Sweden, Borås, Sweden

Received 20 October 2012; accepted 15 April 2013

### Abstract

Nanometer scale surface features on implants and prostheses can potentially be used to enhance osseointegration and may also add further functionalities, such as infection resistance, to the implant. In this study, a nanostructured noble metal coating consisting of palladium, gold and silver, never previously used in bone applications, was applied to machined titanium screws to evaluate osseointegration after 6 and 12 weeks in rabbit tibiae and femurs. Infection resistance was confirmed by *in vitro* adhesion test. A qualitatively and quantitatively similar *in vivo* bone response was observed for the coated and uncoated control screws, using histology, histomorphometry and electron microscopy. The bone-implant interface analysis revealed an extensive bone formation and direct bone-implant contact. These results demonstrate that the nanostructured noble metal coating with antimicrobial properties promotes osseointegration and may therefore be used to add extra implant functionality in the form of increased resistance to infection without the use of antibiotics.

© 2013 Elsevier Inc. All rights reserved.

**Key words:** Titanium; Noble metals; Antimicrobial; Nanotopography; Osseointegration

Implants designed for integration in bone have long been subjected to various types of modifications in order to improve conditions for their integration in the host tissue. Surface topographies on the micrometer scale imposed on the surface of medical devices have been extensively evaluated and have been shown to influence bone response and implant integration.<sup>1</sup> The importance of surface

chemistry and topography on the nanometer scale is not yet well understood, particularly in the complex *in vivo* environment.

Nanostructures, commonly defined as having at least one dimension less than 100 nm, are thought to have a direct impact on biological responses, since the architecture within living systems is constituted by building blocks on the nanoscale. *In vitro* studies have indeed shown effects on bone cells when cultured on a nanostructured surface: these effects include improved cell adherence, a higher degree of differentiated cells and more bone mineralisation.<sup>2–4</sup> The evidence from *in vivo* studies is scarcer, but increased bone-implant contact for nanostructured surfaces compared with smooth ones has been suggested.<sup>5</sup> Furthermore, microtopographically complex surfaces modified with calcium phosphate nanocrystals resulted in increased bone-implant contact.<sup>6</sup> In addition, surfaces with combined topography on the micrometer

Support for research: BIOMATCELL Vinn Excellence Center of Biomaterials and Cell Therapy, supported by VINNOVA and Region Västra Götaland; The Swedish Research Council (grant K2012-52X-09495-25-3); Bactiguard AB; The Hjalmar Svensson foundation; The Felix Neubergh foundation.

\*Corresponding author. Department of Biomaterials, University of Gothenburg, Göteborg, Sweden.

E-mail address: sara.svensson@biomaterials.gu.se (S. Svensson).

1549-9634/\$ – see front matter © 2013 Elsevier Inc. All rights reserved.

<http://dx.doi.org/10.1016/j.nano.2013.04.009>

and nanometer scale displayed increased biomechanical strength compared with surfaces with topography only on the micrometer scale.<sup>7</sup> At the same time, some studies have failed to demonstrate an advantageous effect of nanofeatures in early bone healing around implants, demonstrating the complexity in these studies.<sup>8</sup>

Nanostructures may also be used to add further beneficial properties to the implant. For example, noble metal coatings with a specific nanostructure are of interest due to their ability to resist infections. One example is a noble metal coating consisting of palladium (Pd), gold (Au) and silver (Ag) deposits that are covalently bound to the substrate, providing a surface structure on the nanometer scale. This type of coating has previously been applied to urinary catheters (latex and silicone) and central venous catheters (polyurethane), demonstrating a reduction in the infection rate of up to 50%.<sup>9–11</sup> Depending on the combination of noble metals, these coatings have been shown to modulate inflammation in soft tissue<sup>12</sup> and attenuate coagulation and immune complement activation *in vitro*.<sup>13,14</sup> The antibacterial mode of action of this coating is yet not fully elucidated. Anti-adhesive and galvanic mechanisms have been forwarded, and it appears that the action does not rely on ion- or particle release to the surroundings. The nanostructure (topography) of the coating may also be an important factor.

Infection-resistant implants are of interest due to the difficulty involved in treating infections associated with implanted medical devices. Some attempts have been made to render titanium implants infection resistant. Attempts of this kind are based on hydrophilic surface coatings (e.g. chitosan or polyethylene glycol), the UV-induced photocatalytic effect of crystalline titanium dioxide coatings or the release of antimicrobial agents from coatings (reviewed in Zhao et al 2009).<sup>15</sup> For example, the use of silver and silver ion release is a common approach to provide a surface with antimicrobial activity.<sup>16</sup> In addition to the antimicrobial properties of implanted materials, the exposure of the material surface properties to the biological environment to demonstrate biocompatibility, is equally important. Therefore, both infection resistance and biocompatibility are essential desired properties. Still, information on the *in vivo* performance of these approaches is rare.

Staphylococcal species, *S. aureus* and *S. epidermidis*, are the most common causative agents of biomaterial-associated infections and the number of infections due to virulent antibiotic-resistant strains like methicillin-resistant *S. aureus* (MRSA) are increasing, leaving these patients with fewer treatment options.<sup>17,18</sup> Consequently, infection-resistant implants without the use or incorporation of antibiotics would be of great benefit.

The strategy of this study was to use a functional, infection-resistant, noble metal nanostructured surface from a different medical device application and apply it to titanium implants for bone applications. The aim was to compare the bone response, both qualitatively and quantitatively, between noble metal coated implants and standard, clinically used, machined titanium implants.

## Methods

Additional details are found in the Supplementary Materials.

## Implants

Screw-shaped implants, 4 mm in length and 3.75 mm in external diameter, were manufactured by machining commercially pure (cp) titanium (grade 1). The coating on the implant surface was applied through the Bactiguard® surface treatment technology, which is a wet chemical plating process. The process is carried out in several steps, which create an end result with a mixture of noble metals consisting of silver, gold and palladium. The implants were sterilised by ethylene oxide and contained no detectable endotoxin as measured by the limulus amoebocyte lysate test ( $\leq 0.005$  EU/ml).

## Chemical characterisation of implants

### X-ray photoelectron spectroscopy

X-ray photoelectron spectroscopy (XPS), a surface sensitive chemical analysis technique, was used to obtain information about the chemical composition of the outermost 5 nm layer of the implant surfaces. Relative concentrations of the metallic elements on the sample surfaces were calculated from peak intensities in spectra, after correction by the relative sensitivity factors of the instrument.

## Topographical characterisation of implants

### Scanning electron microscopy

The surface topography of six coated and non-coated implants was qualitatively evaluated using scanning electron microscopy (SEM). Secondary electron images were taken at different magnifications using an in-lens detector for optimal resolution.

### Interferometry

The topography of coated and non-coated implants was quantitatively measured using optical interferometry. Six implants of each type were examined and nine measurements, in the peaks, valleys and flanks of three consecutive threads, were made on each screw. The 3D roughness parameters that were calculated were the arithmetic average height deviation ( $S_a$ ), the density of summits ( $S_{ds}$ ) and the developed surface area ratio ( $S_{dr}$ ).

## Coating adherence on implant surface

In order to evaluate the adherence of the coating to the implants, coated implants ( $n = 24$ ) were subjected to insertion and removal in a rigid polyurethane foam. The noble metal content on the implant and the plastic was analysed by high-resolution inductively coupled mass spectrometry (HR-ICP-MS). Intact sawbone served as reference. Six screws were saved for visual characterisation in SEM.

## Primary bacterial adhesion

Primary adhesion of *Staphylococcus aureus* (ATCC 12600) was evaluated using a modified version of the Ahearn test.<sup>19</sup> Sterilised coated and non-coated implants ( $n = 3$ ) were exposed to  $10^6$ – $10^7$  CFU/ml in PBS in a shaking culture for 24 h at 37°C. Thereafter, the screws were rinsed and the adherent

bacterial cells were detached and evaluated using the viable count technique.

### Surgical procedures

Sixteen adult female New Zealand White rabbits were used in the study. The experiment (including pre-operative, operative and post-operative care and maintenance of the animals) was approved by the local Animal Ethics Committee at the University of Gothenburg, Gothenburg, Sweden (Dnr 306/06). The rabbits were kept at an animal facility, subjected to humane care with daily supervision and free access to food and water. They were housed individually in cubicles one week prior to, and two weeks after surgery, thereafter in groups of eight for the rest of the experiment.

Surgery was performed under sterile conditions. Each rabbit received a total of four implants: two in the femur and two in the tibia; coated implants in one leg and control implants in the other. The placement in the right and left legs was alternated. Animals were anaesthetised with intramuscular injections of a combination of fentanyl and fluanisone and an intraperitoneal injection of diazepam. The bone was exposed through skin incisions and blunt dissection of the underlying tissue including the periosteum. The holes in the bone were prepared using dental implantation drills up to a diameter of 3.5 mm under profuse irrigation with sterile saline. After insertion of implants, the tissue layers and skin were sutured. The analgesic buprenorphine was given twice during three days postoperatively. The combination trimethoprim-sulfamethoxazole was administered preoperatively as well as for five days postoperatively. The implant retrieval was performed after 6 and 12 weeks. The rabbits were sacrificed with an overdose of barbiturate and fixated by perfusion via the left heart ventricle with 2.5% glutaraldehyde in 0.05 M sodium cacodylate buffer. The implants and the surrounding bone were removed *en bloc* and further immersed in glutaraldehyde for 2–4 days.

### Characterisation of bone-implant interface

#### Histology and histomorphometry

The fixated implants with surrounding tissue were dehydrated in graded series of ethanol and embedded in plastic resin. The cured resin-embedded implant was then divided into two pieces through the long axis of the implant by a diamond-coated band saw. Ground sections were prepared from one of the halves by grinding the sections to 15–20  $\mu\text{m}$ . The sections were stained with toluidine blue and were then subjected to histological examination in an optical microscope connected to image analysis software. Histomorphometry included the determination of the bone area within the threads of the screws and the bone-implant contact (BIC). The bone area percentage (bone area/total area) was measured within the threads of the screws, while the bone contact percentage (bone contact/total contact) was measured along the sides of the screws using a 20x magnification objective and a 10x magnification eyepiece. All measurements were performed blinded.

#### Ultrastructural analysis of bone-implant interface

Representative samples of the different implant types and sites were chosen for further implant-tissue interface analysis

Table 1

Relative amount of noble metals found on the screw surfaces.

	Control implants (%)				Coated implants (%)			
Pd	-	-	-	-	3.9	4.3	5.1	4.0
Ag	-	-	-	-	2.6	2.7	2.5	0.2
Au	-	-	-	-	0.5	0.4	0.6	0.4

Relative concentrations (atom %) of palladium (Pd), silver (Ag) and gold (Au) on the surface of control and coated titanium implants (n = 4) as detected by X-ray Photoelectron Spectroscopy (XPS).

with SEM. One part of the *en bloc* embedded implant with surrounding tissue was carefully ground, mounted on SEM holders (with silver glue) and sputter coated with Pd. The samples were then visualised in the backscattered electron mode in a scanning electron microscope.

### Statistics

The interferometer measurements were analysed with one-way ANOVA (n = 6). Histomorphometric parameters were analysed by using the non-parametric Wilcoxon's signed rank test (n = 7–9). All analyses were performed in PASW Statistics 18.0. The confidence level was set at 95%. Results are presented as the mean  $\pm$  standard deviation.

## Results

### Chemical characterisation of implants

#### X-ray photoelectron spectroscopy

The XPS spectra from both the non-coated and coated samples showed strong signals from oxygen (O), titanium (Ti) and carbon (C). The latter most probably originates from organic molecules adsorbed on the surfaces from cleaning solvents, air exposure and possibly also sterile packaging material. High-resolution spectra of the Ti 2p peak showed in all cases a main contribution due to TiO<sub>2</sub> and a weaker contribution due to metallic Ti. The latter indicates that all samples have a TiO<sub>2</sub> surface oxide with a thickness of a few nanometers, in agreement with earlier studies of machined titanium surfaces.<sup>20</sup> The spectra from all the coated samples, but none of the control samples, showed clear signals from Ag, Pd and Au. The relative concentrations (atom %) of noble metals detected in the XPS analyses are shown in Table 1. The amount of noble metals was relatively similar for all coated samples, with the exception of one sample that had a much lower Ag content than the other coated samples.

### Topographical characterisation of implants

#### Scanning electron microscopy

The SEM images showed clear differences in the qualitative surface topography between coated and control implants (Figure 1). The control screws showed ridges and valleys resulting from the machining process at all magnifications, while this pattern was no longer evident on coated screws at magnifications above 5000 x. However, at magnifications up to 1000x, i.e. the 1–10  $\mu\text{m}$  scale, the two implants were indistinguishable, ensuring that the histomorphometric analysis was performed in truly blind fashion. At high magnifications, the

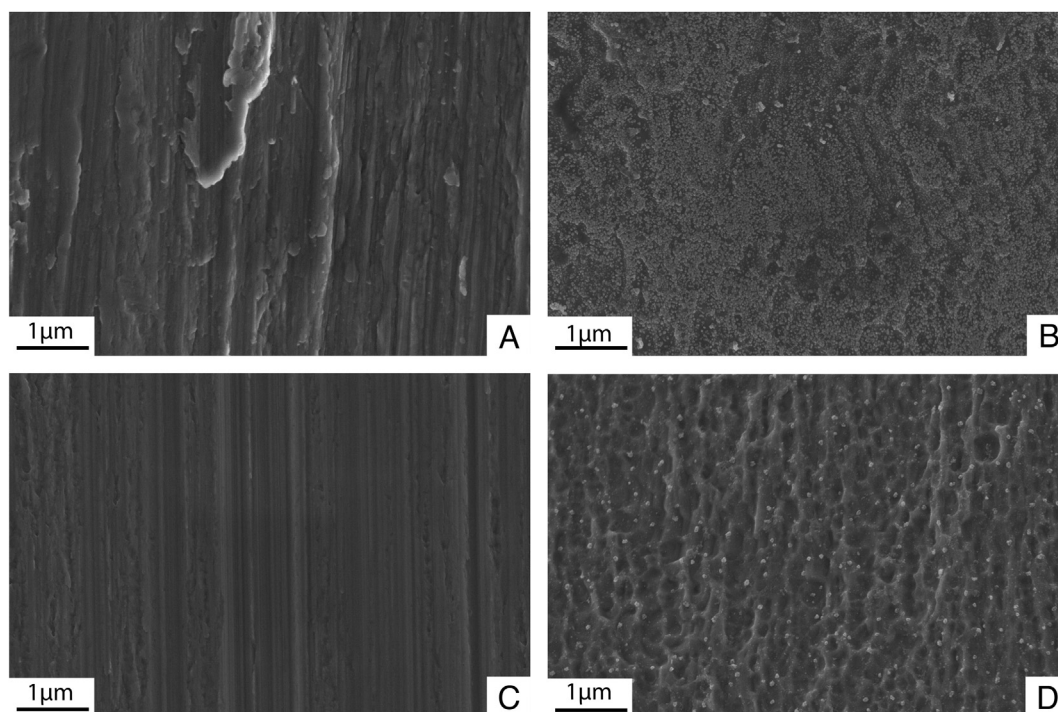


Figure 1. Topographical differences between control and noble metal coated (Pd, Ag, Au) titanium implants as visualised by scanning electron microscopy. Control implants (A, C) showed a typically machined appearance on all parts of the screw, while the coated implants (B, D) had numerous noble metal deposits on the screw surface that dominated the machined appearance at high magnifications. The coating was sparser at the bottom of the threads (D) compared with the upper parts of the threads (B). Magnification 50.000x.

coated samples showed an irregular surface topography on the submicron scale onto which smaller noble metal deposits were dispersed. The deposits varied in size from approximately 10 to 150 nm, with the majority being less than 70 nm in diameter. The deposits were not uniformly distributed along the screw threads. The valleys had fewer and more separated deposits, while the peaks were generally much more densely covered. Many of the coated screws exhibited a gradient of noble deposits on the flanks of the threads, with lower amounts close to the valley and higher amounts close to the peak.

#### Interferometry

The interferometry measurements revealed no statistically significant differences in roughness parameters between coated and control implants (Table 2). A relatively large variation between and within the samples was found for the  $S_a$  values in particular, but also for the  $S_{dr}$  values. This variation was largely dependent on deep ridges in some of the valleys (as well as titanium smears on the implant surfaces). For example, the  $S_a$  values varied between 0.07 and 1.40  $\mu\text{m}$  for individual measurements. Based on the average  $S_a$  values of 0.31 and 0.27  $\mu\text{m}$  for coated and control screws respectively, the implants can be categorised as smooth, although some areas of the screws would be considered minimally ( $S_a$ : 0.5–1  $\mu\text{m}$ ) or even moderately ( $S_a$ : 1–2  $\mu\text{m}$ ) rough.<sup>21</sup>

#### Coating adherence on implant surface

The insertion and removal of the implants in sawbone plastic resulted in a loss of approximately 20–35% of the noble metal

Table 2

Optical interferometry surface roughness.

	$S_a$ ( $\mu\text{m}$ )	$S_{ds}$ ( $\mu\text{m}^{-2}$ )	$S_{dr}$ (%)
Coated	$0.31 \pm 0.31$	$0.14 \pm 0.04$	$6.5 \pm 5.3$
Control	$0.27 \pm 0.20$	$0.12 \pm 0.02$	$5.1 \pm 3.6$

Roughness parameters of noble metal coated and non-coated titanium implants as measured by optical interferometry. Measurements are based on an average of six screws per group; each screw was measured at three different peaks, flanks and valleys. Results are presented as the mean  $\pm$  standard deviation.

content (Table 3). SEM revealed almost unaffected screw valleys, while a large portion of the screw tips were covered with remaining plastic debris. Thread tips not covered by sawbone plastic showed a lower coating coverage, indicating that the coating loss had taken place during the removal of the implant as a result of the sawbone sticking hard to the outer screw layer.

#### *S. aureus* adhesion to implants

According to the modified Ahearn *in vitro* test, the viable counts of the *S. aureus* strain from both trials were  $1.7 \times 10^6$  and  $1.3 \times 10^6$  CFU/implant on the non-coated screws, while only  $8.4 \times 10^3$  and  $1.2 \times 10^4$  CFU/implant adhered to the coated screws. There was a 99% inhibition of adherent bacteria to the coated screws compared to the non-coated (Figure 2).

Table 3  
Durability of coating tested in Sawbone®.

	Pd (µg)	Ag (µg)	Au (µg)
Coated implants prior to test	1.20 ± 0.13	1.01 ± 0.32	0.14 ± 0.01
Sawbone plastic after test	0.30 ± 0.06	0.22 ± 0.07	0.05 ± 0.02
Loss of noble metals	24.9%	21.8%	33.4%

Amounts of palladium (Pd), silver (Ag) and gold (Au) on the surface of coated titanium implants and in Sawbone® plastic after insertion/removal test as measured by inductively coupled plasma mass spectrometry (ICP-MS). Sawbone® control contained <0.01 µg Pd, 0.03 µg Ag and 0.01 µg Au. Results are presented as the mean ± standard deviation (n = 6).

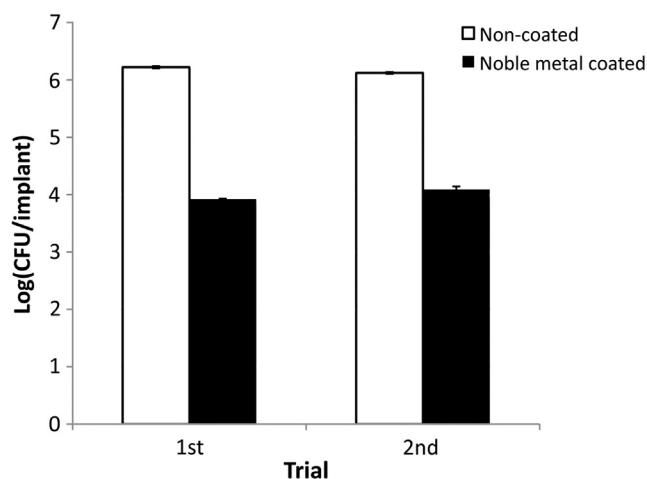


Figure 2. Number of *Staphylococcus aureus* (CFU/implant) adherent to noble metal coated (Pd, Ag, Au) and non-coated titanium screws after 24 h shaking culture in PBS. Inoculation concentration was  $10^6$ – $10^7$  CFU/ml. Results are presented as mean ± standard deviation.

### Biological evaluation of bone response to implants

#### Histology

The bone response to the two different implants was similar in histological terms. In the tibia, the screws were installed in the cortex, with 1 to 2 threads located within the pre-existing bone. New bone was observed originating from the endosteum, extending towards the implant and following the screw contour down into the bone marrow cavity. Approximately 3–4 threads were filled with bone after 6 weeks and 4–6 threads after 12 weeks (Figure 3). Evidence of *de novo* bone formation in the form of bone islands in the matrix (separated from osteoconduction) was detected in the lower threads located in the bone marrow.

In the femur, bone had formed around the implants after just 6 weeks; this included the extension of bone trabeculae towards the implant surface, with an apparent condensation of bone. After 12 weeks, the screws were embedded in even more bone (Figure 4). Periosteal bone formation was seen for the two implant types in both the femur and tibia.

After 6 weeks of implantation, bone formation and remodeling was demonstrated in the femur and tibia, as indicated by

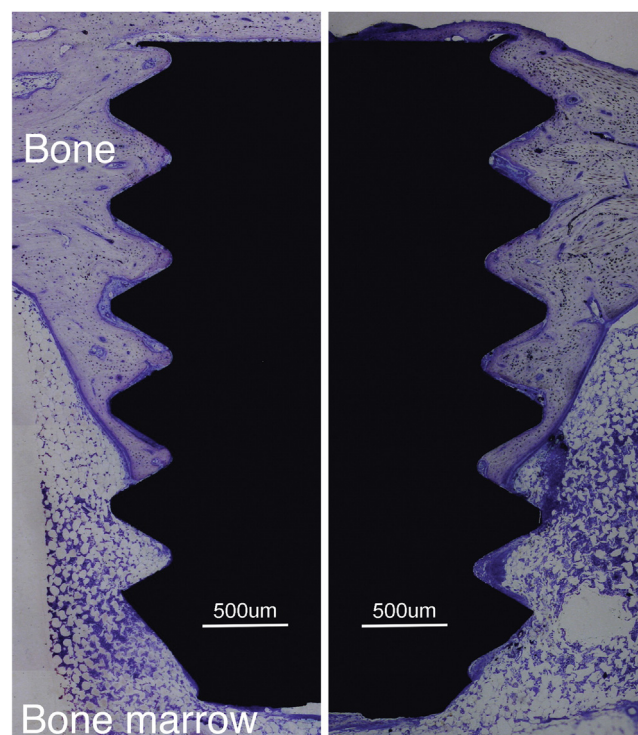


Figure 3. Bone formation in the tibia after 12 weeks of implantation. There was no histological difference between noble metal coated (Pd, Ag, Au) (left) and control (right) implants.

darker stained newly mineralised bone (woven bone) and a large number of osteoblast seams, as well as osteoclasts. After 12 weeks of implantation, most of the bone, especially around the femoral implants, was already remodelled and more closely resembled highly organised lamellar bone. Some active areas could still be seen, especially at the borders between the bone and the marrow and close to the implant surface. No adverse events such as inflammation were detected.

#### Histomorphometry

The bone area percentage within the threads increased over time in both the tibia and femur, but did not differ between coated and control implants (Table 4). The bone-implant contact did not change substantially over time and was similar for the two implant types (Table 5). One exception was found for the bone-implant contact in the femur after 12 weeks, which was significantly lower for the coated screws compared with the controls ( $p = 0.018$ ). Both bone area and bone-implant contact were higher in trabecular bone (femur) compared with cortical bone (tibia) for both coated and control screws.

#### Ultrastructural analysis of bone-implant interface

Ultrastructural analysis with backscattered SEM was used to further analyse the bone in relation to the implants. A large amount of mineralised bone was found filling the threads. Osteocyte lacunae were observed close to the implant surface in all samples. A gap of commonly 1–2 µm was seen between the bone tissue and the implant, as is normally the case for relatively smooth implants.<sup>22,23</sup> However, the bone contour generally followed the screw surface (Figure 5), indicating that direct

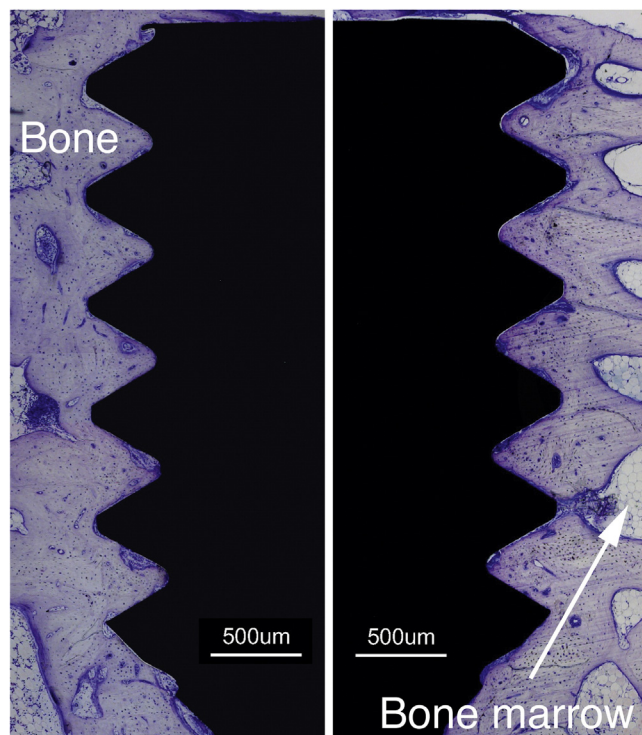


Figure 4. Bone formation in the femur after 12 weeks of implantation. There was no histological difference between noble metal coated (Pd, Ag, Au) (right) and control (left) implants.

contact between bone and implant had been established *in vivo* but had been disturbed during sample preparation. In overall terms, the bone-implant interface was equivalent for coated and control implants.

## Discussion

New generations of biomaterials intended for implantation in the human body are likely to have multiple functions, e.g. to promote the regeneration of tissue and to prevent adverse reactions such as medical device-related infections. One tentative example is orthopaedic prostheses that might benefit from surface modifications that stimulate osseointegration and prevent bacterial adhesion. Strategies to prevent biofilm formation include the promotion of cell adhesion and tissue regeneration on and in close contact with the implant surface,<sup>24</sup> thereby facilitating the host defence and reducing the available surface for microbial adhesion and colonisation. This theory of “race for the surface”<sup>24</sup> is accompanied by the critical observation that bacteria may also reside in the tissue, some distance away from the implant surface.<sup>25</sup> Other lines of defence include local administration of antimicrobial substances to interfere with bacterial survival, cross-talk and biofilm formation.<sup>26</sup>

The results of the present study show that a noble metal coating composed of Pd, Au and Ag, known to reduce infections in extra-osseous clinical applications,<sup>9–11</sup> resulted in an equally high degree of bone-implant contact and amount of regenerated bone as machined c.p. titanium implants, which are used successfully in medicine and dentistry. The study was performed

Table 4  
Bone area around the implants.

	Femur (%)		Tibia (%)	
	6 weeks	12 weeks	6 weeks	12 weeks
Coated	75 ± 9.1	82 ± 3.3	40 ± 9.0	57 ± 4.7
Control	78 ± 3.9	85 ± 3.6	46 ± 5.2	54 ± 19

Bone area (%) measured as the area within the threads along the sides of the screw implant on histological sections using light microscopy. Results are presented as the mean ± standard deviation.

Table 5  
Bone-implant contact (BIC).

	Femur (%)		Tibia (%)	
	6 weeks	12 weeks	6 weeks	12 weeks
Coated	33 ± 8.8	26 ± 8.1	17 ± 7.0	17 ± 8.1
Control	33 ± 11	36 ± 8.6	19 ± 5.8	18 ± 5.4

BIC (%) measured along the sides of the screw implant on histological sections using light microscopy. Results are presented as the mean ± standard deviation.

using an experimental model that allows the detection of material surface modifications that lead to either improved or reduced bone-implant contact and bone bonding.<sup>27,28</sup> In addition, *in vitro* tests showed 99% inhibition of *S. aureus* adhesion on coated compared to non-coated implants.

There are few *in vivo* studies that have focused on the effect of single and combined noble metals on bone regeneration in association with implanted medical devices. A reduction in the osseointegration of implants composed of pure gold, which normally lacks a surface oxide,<sup>29,30</sup> indicated that the properties of oxides may play an important role in osseointegration.<sup>31</sup> In the present study, the dominant surface elements detected by the surface sensitive technique XPS were titanium and oxygen, titanium being in the form of a TiO<sub>2</sub> surface oxide, for both noble metal coated titanium (test) and titanium (control) screws. Furthermore, ultrastructural observations revealed a qualitatively different topography but a similar quantitative surface roughness value on the micron scale, as judged by quantitative interferometry. Prominent features of the coated titanium implants were the presence of small amounts (<1 μg cm<sup>-2</sup>) of Pd, Au and Ag in the form of 10–150 nm metal deposits that formed a distinct nanotopography. Although the metal deposits appeared to be more numerous on the outer parts of the threads, in contrast to the more scarce distribution in the valleys, this difference did not seem to affect the local bone response, since the bone-implant contact at the peaks of the screw threads appeared similar for both implants. Interestingly, in one *in vitro* study, bone cell adhesion and proliferation onto surfaces exhibiting a gradient of nanoparticles was reduced when the particle density was high.<sup>32</sup> Moreover, in another study, it was shown that disordered nanostructures increased osteoblast differentiation *in vitro*.<sup>33</sup> Notably, for coated implants, the underlying machined titanium topography was less evident. However, despite this qualitative difference in topography between coated and control implants, the interferometry measurements did not reveal any quantitative difference in roughness in terms of S<sub>a</sub> values.

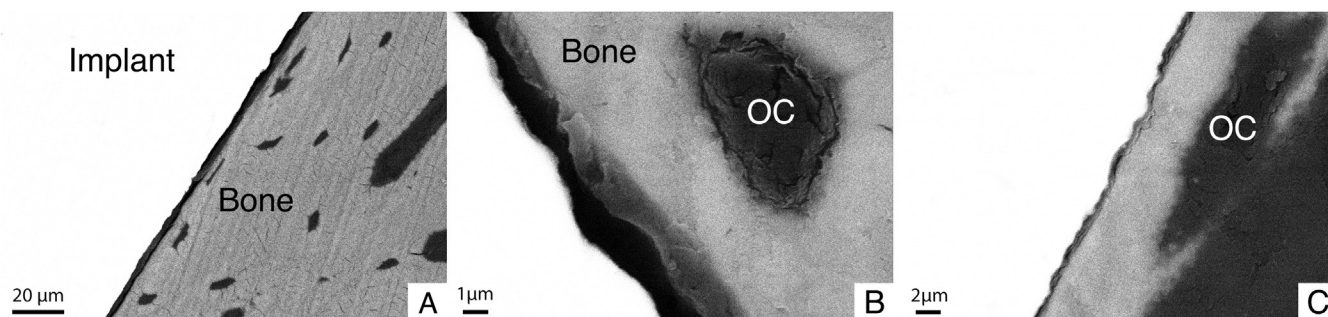


Figure 5. Backscattered scanning electron microscopy was used to evaluate the ultrastructure of the bone-implant interface. Several osteocytes were seen trapped within the bone close to the bone-implant interface. A gap, 1–2  $\mu\text{m}$  wide, was seen between the implant and the bone. However, the bone edge follows the screw contour, indicating that direct contact between tissue and implant was established after implantation. (A) control, tibia, 12 weeks; (B) control, tibia, 12 weeks; (C) noble metal coated (Pd, Ag, Au), tibia, 6 weeks. OC = osteocyte.

The combination of altered chemistry and surface topography presents major difficulties when it comes to interpreting the specific surface property (chemistry vs. micro- and nanotopography) that played the most important role for the current *in vivo* observations. A change in one material surface-related variable may lead to other chemical and/or topographical changes. For example, coatings or treatments that generate nanostructures onto a biomaterial added a completely different chemistry to the surface, e.g. hydroxyapatite (HA), other calcium phosphates (CaP) or poly-lactic-co-glycolic acid (PLGA),<sup>6,34</sup> thus leaving the question of whether it was the topography or the chemistry that caused the changes in the cell or tissue response. In a study by Meirelles et al, the authors tried to separate the chemistry from the nanotopographic structures by making ultra-smooth titanium surfaces with either HA nanocrystals or titania nanostructures.<sup>5</sup> The authors demonstrated that the bone-implant contact was higher with nano-titania after 4 weeks of implantation in rabbit tibia and suggested that bone healing was more dependent on the size and distribution of nanofeatures than on the chemistry. On the other hand, it is assumed that, on the nano-scale and beyond, certain properties of the material surface will inevitably change compared with the same material in the bulk phase. For example, properties such as charge, conductivity, roughness, porosity, wettability and friction, as well as physical and chemical reactivity, can be influenced by the nanostructuring of a surface.<sup>35</sup> This implies that, even though the same material (e.g. Ti) is used as nanostructures, the properties of the surface will nonetheless be different. The protein affinity for the surface will be altered, which will in turn affect the cell adhesion and behaviour at the material surface.<sup>36,37</sup> It is known that material surface chemistry and microtopography have synergistic effects, with respect to osteoblast differentiation, for example.<sup>38</sup> It is therefore possible that the nanotopography and the chemistry of a surface also act in synergy and provide properties that promote or inhibit osteogenesis, as well as influence bacterial adhesion and colonisation.

The bone response to the two types of surfaces studied here was very similar, as demonstrated by the large amount of newly formed bone around the implants and in contact with the implant surface after 6 weeks and increasing up to 12 weeks. The difference in bone-implant contact between coated and non-coated implants in the femur after 12 weeks was the only significant observation. An explanation might be an increased

bone remodelling in the proximity of the surface. Although a negative effect of the coating cannot be excluded, no such assumption was verified by the histological examination after 12 weeks, which excluded adverse events such as inflammation or bone resorption localised at the surface of the implants. To examine possible noble metal particle release from the coating, an *in vitro* bench-test in Sawbone<sup>®</sup> plastic resembling the density and structure of the compact tibial cortex was performed. The test is presumed as a worst-case scenario, being performed in a dry environment with both insertion and removal of the implants in non-pre-threaded holes with a smaller diameter than the screws. Hence, the observed result that 20–35% of the coating was lost to the plastic can be assumed to be an overestimation of what would take place in an *in vivo* situation, and still the majority of the coating was intact. Gosheger et al implanted silver-releasing implants in rabbit femur and found that the mean silver concentration was 1.88 ppb in blood and 90.4 ppb in the liver, but no pathological findings were made.<sup>39</sup> The permissible exposure limit is 0.01  $\text{mg}/\text{m}^3$  for both ionic and elemental silver, although metallic silver appears to be less toxic.<sup>40</sup> However, since the noble metal coating used in the present study contain very small amounts of metallic silver ( $<0.5 \mu\text{g}/\text{cm}^2$ ), very low concentrations of potentially released silver in the body could be expected. Furthermore, previous studies using similar noble metal (Pd, Au, Ag) coatings *in vitro*<sup>41</sup> and in soft tissues<sup>12</sup> have demonstrated cyto- and biocompatibility. In addition, the lack of difference between the two implant types in the tibia contradicts the possibility that the noble metal coating would have adversely affected osseointegration. Nevertheless, the observed reduction in bone-implant contact in the femur after 12 weeks implies that additional future studies with longer implantation should be considered. Furthermore, biomechanical evaluation is important prior to clinical trials.

The fact that osseointegration was achieved for titanium implants with added anti-infectious functionality in the form of a nano-scale metal coating provides a strong reason to examine the role of surface immobilised nanoparticles of specific chemistry for osteogenesis, as well as host defence and microbial adhesion. Most likely, a focus of this kind requires both *in vitro* and *in vivo* approaches. Previous studies in these directions have mainly focused on osteoblast behaviour in relation to different releasing or non-releasing silver-containing materials, showing no cytotoxic

effect.<sup>42–45</sup> Many of these studies revealed strong *in vitro* antimicrobial properties and osteogenic maturation was stimulated by low concentrations of elementary silver.<sup>44</sup> In contrast, a tendency towards reduced cell growth and significantly depressed alkaline phosphatase activity was seen in the case of osteoblasts cultured in the presence of a silver wire.<sup>46</sup> Effects of silver ions on bone regeneration *in vivo* are less well studied. Silver-coated endoprostheses inserted in a rabbit infection model were associated with a significantly reduced infection rate (40%), lower signs of inflammation and the absence of toxicological side-effects in the silver group.<sup>39</sup> However, osseointegration was not assessed. In a clinical study over a 5-year period, the infection rate was reduced from 17.6% in sarcoma patients (femur and tibia) with a titanium megaprosthesis to 5.9% in patients with a silver megaprosthesis.<sup>47</sup> The literature on the effect of gold and palladium on osteoblast behaviour is scarcer than for silver. A few studies evaluating gold and/or palladium materials have shown good biocompatibility for osteoblast attachment, growth and differentiation<sup>46,48</sup> and, to some extent, improved long-term osteoblast adhesion when cultured on gold-palladium sputtered titanium and stainless steel.<sup>49</sup>

For bone-implant applications intended for long-term use, it is essential that the implants with alleged antibacterial properties, irrespective of their mechanism of action, achieve osseointegration. If this is not achieved, the lack of stability will most likely deteriorate the function of the implant and clinical performance. A close bond between the titanium and the bone tissue may impede bacterial adhesion, colonisation and biofilm formation.<sup>50</sup> Consequently, bone implants that are not well osseointegrated are presumably more susceptible to infections. According to the results obtained in this study, titanium implants with a noble metal coating demonstrate osseointegration, with the added potential benefit of preventing and/or reducing device-related infections. Future studies of noble metal coatings in orthopaedic and dental applications are needed in order to elucidate their ability to resist infection and to promote and maintain osseointegration.

In conclusion, the bone response to the nanostructured noble metal coated titanium implants, which possessed anti-adhesive properties to *S. aureus in vitro*, was qualitatively and quantitatively very similar to that of standard, clinically used machined titanium screws, which become osseointegrated. These results indicate that the coating does not impede osseointegration and may thus be used to add extra implant functionality in the form of increased resistance to infection without the use of antibiotics. This could be of interest when it comes to reducing the infection risk in high-risk and compromised patients or in implant systems where the titanium implant penetrates the skin or the mucosa. However, future studies are needed to assess osseointegration and antimicrobial activity of the implants in compromised bone-implant healing situations, e.g. in an implant infection model.

## Acknowledgments

We sincerely thank Victoria Fröjd for her help with the interferometry measurements and Billy Södervall for performing the noble metal coating of the implants.

## Appendix A. Supplementary data

Supplementary data to this article can be found online at <http://dx.doi.org/10.1016/j.nano.2013.04.009>.

## References

1. Wennerberg A, Albrektsson T. Effects of titanium surface topography on bone integration: a systematic review. *Clin Oral Implants Res* 2009;**20**:172–84.
2. Dalby MJ, McCloy D, Robertson M, Agheli H, Sutherland D, Affrossman S, et al. Osteoprogenitor response to semi-ordered and random nanotopographies. *Biomaterials* 2006;**27**:2980–7.
3. Webster TJ, Ejirofor JU. Increased osteoblast adhesion on nanophase metals: Ti, Ti6Al4V, and CoCrMo. *Biomaterials* 2004;**25**:4731–9.
4. de Oliveira PT, Nanci A. Nanotexturing of titanium-based surfaces upregulates expression of bone sialoprotein and osteopontin by cultured osteogenic cells. *Biomaterials* 2004;**25**:403–13.
5. Meirelles L, Melin L, Peltola T, Kjellin P, Kangasniemi I, Currie F, et al. Effect of hydroxyapatite and titania nanostructures on early *in vivo* bone response. *Clin Implant Dent Relat Res* 2008;**10**:245–54.
6. Mendes VC, Moineddin R, Davies JE. Discrete calcium phosphate nanocrystalline deposition enhances osteoconduction on titanium-based implant surfaces. *J Biomed Mater Res A* 2009;**90**:577–85.
7. Kubo K, Tsukimura N, Iwasa F, Ueno T, Saruwatari L, Aita H, et al. Cellular behavior on TiO<sub>2</sub> nanonodular structures in a micro-to-nanoscale hierarchy model. *Biomaterials* 2009;**30**:5319–29.
8. Schouten C, Meijer GJ, van den Beucken JJ, Leeuwenburgh SC, de Jonge LT, Wolke JG, et al. *In vivo* bone response and mechanical evaluation of electrosprayed CaP nanoparticle coatings using the iliac crest of goats as an implantation model. *Acta Biomater* 2010;**6**:2227–36.
9. Goldschmidt H, Hahn U, Salwender HJ, Haas R, Jansen B, Wolbring P, et al. Prevention of catheter-related infections by silver coated central venous catheters in oncological patients. *Zentralbl Bakteriol* 1995;**283**:215–23.
10. Karchmer TB, Giannetta ET, Muto CA, Strain BA, Farr BM. A randomized crossover study of silver-coated urinary catheters in hospitalized patients. *Arch Int Med* 2000;**160**:3294–8.
11. Schumm K, Lam Thomas BL. Types of urethral catheters for management of short-term voiding problems in hospitalised adults. *Cochrane Database Syst Rev [serial on the Internet]* 2008;**1,2**(2) Available from: <http://www.mrw.interscience.wiley.com/cochrane/clsystrev/articles/CD004013/frame.html>.
12. Suska F, Svensson S, Johansson A, Emanuelsson L, Karlholm H, Ohrlander M, et al. *In vivo* evaluation of noble metal coatings. *J Biomed Mater Res B Appl Biomater* 2010;**92**:86–94.
13. Hulander M, Hong J, Andersson M, Gerven F, Ohrlander M, Tengvall P, et al. Blood interactions with noble metals: coagulation and immune complement activation. *ACS Appl Mater Interfaces* 2009;**1**:1053–62.
14. Hulander M, Lundgren A, Berglin M, Ohrlander M, Lausmaa J, Elwing H. Immune complement activation is attenuated by surface nanotopography. *Int J Nanomedicine* 2011;**6**:2653–66.
15. Zhao L, Chu PK, Zhang Y, Wu Z. Antibacterial coatings on titanium implants. *J Biomed Mater Res B Appl Biomater* 2009;**91**:470–80.
16. Juan L, Zhimin Z, Anchun M, Lei L, Jingchao Z. Deposition of silver nanoparticles on titanium surface for antibacterial effect. *Int J Nanomedicine* 2010;**5**:261–7.
17. Pulido L, Ghanem E, Joshi A, Purtill JJ, Parvizi J. Periprosthetic joint infection: the incidence, timing, and predisposing factors. *Clin Orthop Relat Res* 2008;**466**:1710–5.
18. Walls RJ, Roche SJ, O'Rourke A, McCabe JP. Surgical site infection with methicillin-resistant *Staphylococcus aureus* after primary total hip replacement. *J Bone Joint Surg Br* 2008;**90**:292–8.
19. Gabriel MM, Sawant AD, Simmons RB, Ahearn DG. Effects of silver on adherence of bacteria to urinary catheters: *in vitro* studies. *Curr Microbiol* 1995;**30**:17–22.



20. Lausmaa J. Surface spectroscopic characterization of titanium implant materials. *J Electron Spectrosc Relat Phenomena* 1996;**81**:343-61.
21. Albrektsson T, Wennerberg A. Oral implant surfaces: Part 1 – review focusing on topographic and chemical properties of different surfaces and in vivo responses to them. *Int J Prosthodont* 2004;**17**:536-43.
22. Palmquist A, Lindberg F, Emanuelsson L, Branemark R, Engqvist H, Thomsen P. Morphological studies on machined implants of commercially pure titanium and titanium alloy (Ti6Al4V) in the rabbit. *J Biomed Mater Res B Appl Biomater* 2009;**91**:309-19.
23. Palmquist A, Lindberg F, Emanuelsson L, Branemark R, Engqvist H, Thomsen P. Biomechanical, histological, and ultrastructural analyses of laser micro- and nano-structured titanium alloy implants: a study in rabbit. *J Biomed Mater Res A* 2010;**92**:1476-86.
24. Gristina AG. Biomaterial-centered infection: microbial adhesion versus tissue integration. *Science* 1987;**237**:1588-95.
25. Broekhuizen CA, de Boer L, Schipper K, Jones CD, Quadir S, Feldman RG, et al. Peri-implant tissue is an important niche for *Staphylococcus epidermidis* in experimental biomaterial-associated infection in mice. *Infect Immun* 2007;**75**:1129-36.
26. Bruellhoff K, Fiedler J, Moller M, Groll J, Brenner RE. Surface coating strategies to prevent biofilm formation on implant surfaces. *Int J Artif Organs* 2010;**33**:646-53.
27. Larsson C, Thomsen P, Aronsson BO, Rodahl M, Lausmaa J, Kasemo B, et al. Bone response to surface-modified titanium implants: studies on the early tissue response to machined and electropolished implants with different oxide thicknesses. *Biomaterials* 1996;**17**:605-16.
28. Mohammadi S, Esposito M, Hall J, Emanuelsson L, Krozer A, Thomsen P. Long-term bone response to titanium implants coated with thin radiofrequency magnetron-sputtered hydroxyapatite in rabbits. *Int J Oral Maxillofac Implants* 2004;**19**:498-509.
29. Thomsen P, Larsson C, Ericson LE, Sennerby L, Lausmaa J, Kasemo B. Structure of the interface between rabbit cortical bone and implants of gold, zirconium and titanium. *J Mater Sci Mater Med* 1997;**8**:653-65.
30. Zainali K, Danscher G, Jakobsen T, Jakobsen SS, Baas J, Moller P, et al. Effects of gold coating on experimental implant fixation. *J Biomed Mater Res A* 2009;**88**:274-80.
31. Lausmaa J. Mechanical, thermal, chemical and electrochemical surface treatment of titanium. In: Brunette D, Tnegvall P, Thomsen P, Textor M, editors. *Titanium in medicine*. Heidelberg, Germany: Springer Verlag; 2001.
32. Kunzler TP, Huwiler C, Drobek T, Voros J, Spencer ND. Systematic study of osteoblast response to nanotopography by means of nanoparticle-density gradients. *Biomaterials* 2007;**28**:5000-6.
33. Dalby MJ, Gadegaard N, Tare R, Andar A, Riehle MO, Herzyk P, et al. The control of human mesenchymal cell differentiation using nanoscale symmetry and disorder. *Nat Mater* 2007;**6**:997-1003.
34. Smith LJ, Swaim JS, Yao C, Haberstroh KM, Nauman EA, Webster TJ. Increased osteoblast cell density on nanostructured PLGA-coated nanostructured titanium for orthopedic applications. *Int J Nanomedicine* 2007;**2**:493-9.
35. Riehemann K, Schneider SW, Luger TA, Godin B, Ferrari M, Fuchs H. Nanomedicine – challenge and perspectives. *Angew Chem Int Edit* 2009;**48**:872-97.
36. Tang L, Eaton JW. Fibrin(ogen) mediates acute inflammatory responses to biomaterials. *J Exp Med* 1993;**178**:2147-56.
37. Wu Y, Simonovsky FI, Ratner BD, Horbett TA. The role of adsorbed fibrinogen in platelet adhesion to polyurethane surfaces: a comparison of surface hydrophobicity, protein adsorption, monoclonal antibody binding, and platelet adhesion. *J Biomed Mater Res A* 2005;**74**:722-38.
38. Liao H, Andersson AS, Sutherland D, Petronis S, Kasemo B, Thomsen P. Response of rat osteoblast-like cells to microstructured model surfaces in vitro. *Biomaterials* 2003;**24**:649-54.
39. Gosheger G, Harges J, Ahrens H, Streitburger A, Buerger H, Erren M, et al. Silver-coated megaendoprostheses in a rabbit model—an analysis of the infection rate and toxicological side effects. *Biomaterials* 2004;**25**:5547-56.
40. Drake PL, Hazelwood KJ. Exposure-related health effects of silver and silver compounds: a review. *Ann Occup Hyg* 2005;**49**:575-85.
41. Suska F, Svensson S, Johansson A, Emanuelsson L, Ohlander M, Thomsen P. Noble metals as new antimicrobial and biocompatible coatings. *Clin Oral Implants Res [Abstract]* 2007;**18**:cxliii-cxliv.
42. Alt V, Bechert T, Steinrucke P, Wagener M, Seidel P, Dingeldein E, et al. An in vitro assessment of the antibacterial properties and cytotoxicity of nanoparticulate silver bone cement. *Biomaterials* 2004;**25**:4383-91.
43. Ewald A, Gluckermann SK, Thull R, Gbureck U. Antimicrobial titanium/silver PVD coatings on titanium. *Biomed Eng Online* 2006;**5**:22.
44. Harges J, Streitburger A, Ahrens H, Nusselt T, Gebert C, Winkelmann W, et al. The influence of elementary silver versus titanium on osteoblasts behaviour in vitro using human osteosarcoma cell lines. *Sarcoma* 2007;**2007**:26539.
45. Zheng X, Chen Y, Xie Y, Ji H, Huang L, Ding C. Antibacterial property and biocompatibility of plasma sprayed hydroxyapatite/silver composite coatings. *J Therm Spray Techn* 2009:1-6.
46. Cortizo MC, De Mele MF, Cortizo AM. Metallic dental material biocompatibility in osteoblastlike cells: correlation with metal ion release. *Biol Trace Elem Res* 2004;**100**:151-68.
47. Harges J, von Eiff C, Streitburger A, Balke M, Budny T, Henrichs MP, et al. Reduction of periprosthetic infection with silver-coated mega-prostheses in patients with bone sarcoma. *J Surg Oncol* 2010;**101**:389-95.
48. Lee YH, Bhattarai G, Aryal S, Lee NH, Lee MH, Kim TG, et al. Modified titanium surface with gelatin nano gold composite increases osteoblast cell biocompatibility. *Appl Surf Sci* 2010;**256**:5882-7.
49. Anselme K, Bigerelle M. Effect of a gold-palladium coating on the long-term adhesion of human osteoblasts on biocompatible metallic materials. *Surf Coat Tech* 2006;**200**:6325-30.
50. Tillander J, Hagberg K, Hagberg L, Branemark R. Osseointegrated titanium implants for limb prostheses attachments: infectious complications. *Clin Orthop Relat Res* 2010;**468**:2781-8.